Photosynth Res (2008) 95:55–62
DOI 10.1007/s11120-007-9228-3

REGULAR PAPER

Vibrational mode frequency calculations of chlorophyll-*d* for assessing (P740^{+}-P740) FTIR difference spectra obtained using photosystem I particles from *Acaryochloris marina*

Gary Hastings · Ruili Wang

Received: 14 May 2007 / Accepted: 16 July 2007 / Published online: 21 August 2007

Abstract *Acaryochloris marina* is an oxygen-evolving organism that utilizes chlorophyll-*d* for light induced photochemistry. In photosystem I particles from *Acaryochloris marina*, the primary electron donor is called P740, and it is thought that P740 consist of two chlorophyll-*d* molecules. (P740^{+}-P740) FTIR difference spectra have been produced, and vibrational features that are specific to chlorophyll-*d* (and not chlorophyll-*a*) were observed, supporting the idea that P740 consists chlorophyll-*d* molecules. Although bands in the (P740^{+}-P740) FTIR difference spectra were assigned specifically to chlorophyll-*d*, how these bands shifted, and how their intensities changed, upon cation formation was never considered. Without this information it is difficult to draw unambiguous conclusions from the FTIR difference spectra. To gain a more detailed understanding of cation induced shifting of bands associated with vibrational modes of P740 we have used density functional theory to calculate the vibrational properties of a chlorophyll-*d* model in the neutral, cation and anion states. These calculations are shown to be of considerable use in interpreting bands in (P740^{+}-P740) FTIR difference spectra. Our calculations predict that the 3^1 formyl C–H mode of chlorophyll-*d* upshifts/downshifts upon cation/anion formation, respectively. The mode intensity also decreases/increases upon cation/anion formation, respectively. The cation induced bandshift of the 3^1 formyl C–H mode of chlorophyll-*d* is also strongly dependant on the dielectric environment of the chlorophyll-*d* molecules. With this new knowledge we reassess the interpretation of bands that were assigned to 3^1 formyl C–H modes of chlorophyll-*d* in (P740^{+}-P740) FTIR difference spectra. Considering our calculations in combination with (P740^{+}-P740) FTIR DS we find that the most likely conclusions are that P740 is a dimeric Chl-*d* species, in an environment of low effective dielectric constant (~2–8). In the P740^{+} state, charge is asymmetrically distributed over the two Chl-*d* pigments in a roughly 60:40 ratio.

Keywords Chlorophyll · Chlorophyll-*d* · Density functional theory · Fourier transform infrared · Normal-mode · Vibrational frequencies · Formyl group

Abbreviations

A.	*Acharyochloris*
C=O	carbonyl
Chl-*d, a*	chlorophyll-*d*, *a*
DFT	Density functional theory
DS	Difference spectrum, spectra, spectroscopic or spectroscopy
DDS	Double difference spectrum
FTIR	Fourier transform infrared
PS I	Photosystem I
S6803	*Synechocystis* sp. 6803

Introduction

Acharyochloris (*A.*) *marina* is a recently discovered oxygenic photosynthetic marine prokaryote that utilizes chlorophyll-*d* (Chl-*d*) for light-induced photochemistry (Miyashita et al. 1996, 1997). A structural model for Chl-*d*

Electronic supplementary material The online version of this article (doi:10.1007/s11120-007-9228-3) contains supplementary material, which is available to authorized users.

G. Hastings (✉) · R. Wang
Department of Physics and Astronomy,
Georgia State University, Atlanta, GA 30303, USA
e-mail: ghastings@gsu.edu

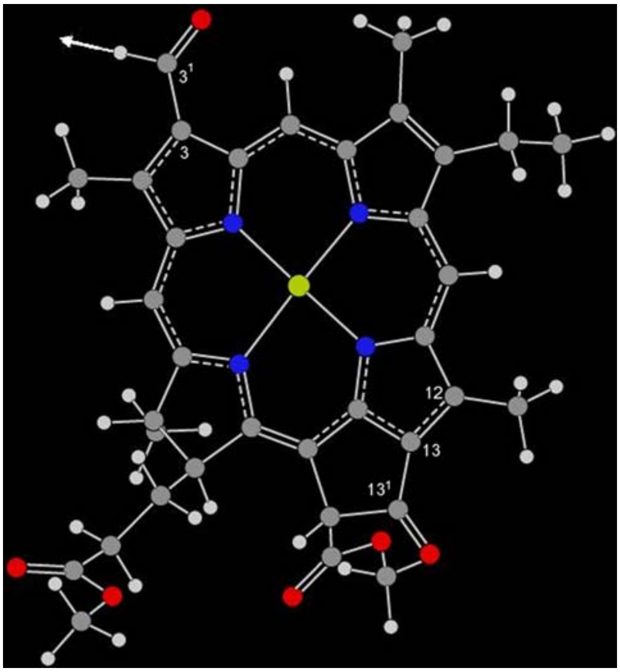

Fig. 1 Structure of the Chl-*d* model used in DFT based calculations. The phytyl tail has been replaced by a methyl group at the 17^3 ester oxygen. Part of the IUPAC numbering scheme is shown, and is used throughout this manuscript. The white arrow shows the atomic motions for the calculated 2,931 cm^{-1} vibrational mode. Clearly, it is a pure C–H stretching mode

is shown in Fig. 1 (without the phytyl chain). Chl-*d* differs from Chl-*a* only in that it contains a formyl group rather than a vinyl group at the 3^1 position (see numbering in Fig. 1). It is the vibrational properties of this formyl group that can therefore be used to distinguish Chl-*d* from Chl-*a* in FTIR difference spectra (DS). In this manuscript we focus specifically on the vibrational features of this formyl group.

Recently, photosystem I (PS I) complexes from *A. marina* have been isolated (Hastings 2001; Hu et al. 1998; Sivakumar et al. 2003). The primary electron donor in PS I from *A. marina* is called P740, because upon illumination a bleaching is observed near 740 nm (Hastings 2001; Hu et al. 1998) in much the same way that a bleaching is observed near 700 nm for P700 found in plants and bacteria. The Q_y absorption maxima for Chl-*d* occurs near 708 nm, which is dramatically red-shifted relative to the corresponding band for Ch-*a*, that occurs near 665 nm. Since P740 displays a dramatically red shifted bleaching relative to P700 it was suggested that P740 was a dimer of Chl-*d* molecules (Hu et al. 1998). Comparison of ENDOR spectra of $P700^+$ and $P740^+$ may also suggest that P740 is a dimer of Chl-*d* molecules (Mino et al. 2005). Later, P740 was suggested to be a heterodimer of Chl-*d* and Chl-*d′* molecules, in the same way that P700 is a heterodimer of Chl-*a* and Chl-*a′* molecules (Akiyama et al. 2001, 2002a, b).

Recently, Sivakumar et al. (2003) have produced light induced ($P740^+$-P740) FTIR difference spectra (DS). In the ($P740^+$-P740) FTIR DS bands were observed that are most likely associated with formyl C–H modes of Chl-*d*, suggesting directly that P740 consists of Chl-*d* molecules. It was further suggested that one of the formyl C-H modes upshifted 8 cm^{-1} upon cation formation (Sivakumar et al. 2003). This was merely a hypothesis that needs to be tested, however. So, although bands in the ($P740^+$-P740) FTIR difference spectra were assigned specifically to Chl-*d*, how these bands shifted, and how their intensities changed, upon cation formation is not known. Without this information it is impossible to draw unambiguous conclusions from the ($P740^+$-P740) FTIR difference spectra. In fact, it was this lack of knowledge of how bands shift (up or down) upon cation formation that led Heald et al. (1988) to the erroneous conclusion that $P700^+$ could be an enol form of Chl-a^+. In the words of Heald et al. (1988): “A large upshift of the keto C=O (of Chl-*a*) from 1,687 to 1,717 cm^{-1} seams unlikely especially in light of the small spin density changes seen at the keto C_9 and the O_1.” It was later shown that such a large upshift of the keto C=O mode of Chl-*a* upon cation formation is indeed likely (Nabedryk et al. 1990), and that the “enol hypothesis” is unnecessary.

Clearly, there is a demonstrated need for FTIR spectra of Chl-*d* and Chl-d^+. In the absence of experimental data, however, quantum chemical calculations are now sufficiently sophisticated to be able to accurately model the vibrational properties of chlorophyll molecules. Indeed, we have recently used density functional theory to calculate the complete set of harmonic vibrational mode frequencies of several Chl-*a* models in both the neutral and cation state (Wang et al. 2007). The calculations on Chl-*a* reported by Wang et al. (2007) can be of use in comparing to the calculated results for Chl-*d* that are reported here.

Previously, Chen et al. (2004) have produced resonance Raman spectra of isolated Chl-*d* at 77 K. They then used density functional theory to calculate the non-resonance Raman active modes of a Chl-*d* model molecular system that lacked the phytyl chain. Presumably these calculations were also undertaken at 77 K although this was never specified, and our calculations suggest otherwise (see below). Chen et al. (2004) did not present calculated Raman spectra. For completeness and to provide a link to the work of Chen et al. (2004), in the supplementary information section we present our calculated Raman spectra at 298 K for a Chl-*d* model molecule that is identical to that studied by Chen et al. (2004). Furthermore, Chen et al. (2004) appear to have clearly assigned a band to the 13^3 ester C=O mode of Chl-*d*. As we explained previously such an assignment is not possible for Chl-*a*, as the 13^3 ester C=O and 13^1 keto C=O modes are strongly coupled. We also find a very similar result for Chl-*d*, and cannot assign a mode solely to the 13^3 ester C=O group of Chl-*d*.

It is not entirely clear to what degree calculated non-resonance Raman spectra are useful for analysis of experimental resonance enhanced Raman spectra. In addition, it is unlikely that useful Raman spectra will be obtained for an actual Chl-*d* containing photosynthetic system. This is especially true for the case of Chl-d^+. Given this, calculated non-resonance Raman spectra of Chl-*d* are of limited usefulness. In contrast, cation minus neutral FTIR difference spectra of Chl-*d* containing photosynthetic systems have already been obtained (Hastings 2001; Sivakumar et al. 2003) and it is instructive to compare calculated IR difference spectra to experimental FTIR difference spectra.

In this paper we use density functional theory to calculate (Chl-d^+-Chl-*d*) FTIR difference spectra. We then relate the calculated spectra to experimental ($P740^+$-P740) FTIR difference spectra. Finally, we use our calculations to make predictions about what could be investigated in future FTIR studies of PS I from *A. marina*.

Materials and methods

Molecular geometry optimizations and harmonic vibrational mode frequency calculations were performed using hybrid DFT methods, employing the B3LYP functional and the 6–31G(d) method within Gaussian 03 (Frisch et al. 2004). At this level of theory, computed harmonic vibrational mode frequencies overestimate experimental anharmonic frequencies by approximately 5% (Wheeler 2001). Radical induced frequency shifts and isotope induced frequency shifts are accurately calculated, however (Bandaranayake et al. 2006a; Wang et al. 2007). No negative frequencies were calculated for any of the model molecular structures discussed here. To model solvent effects the integral equation formalism (IEF) of the polarizable continuum model (PCM) was used (Cances et al. 1997, 1999; Mennucci and Tomasi 1997; Tomasi et al. 2002, 2005, 1999), as implemented in Gaussian 03.

Our assignment of calculated vibrational frequencies to molecular groups is somewhat subjective. Here we approximately assign molecular vibrational modes by visual identification of the molecular groups that most prominently contribute to the vibration. This visual identification is performed using the software GaussView 03 in which each of the vibrational motions can be animated and displayed (see Fig. 1).

In this manuscript, both normal mode frequencies and intensities are calculated. This information allows the construction of infrared (IR) "stick spectra". By convolving these "stick" spectra with a Guassian function of 4 cm^{-1} bandwidth, more realistic looking IR spectra are obtained, which we will call absorption spectra. This type of spectral representation is very helpful, as only the vibrational modes with highest intensity are clearly depicted.

Results and discussion

The 3^1 formyl C–H mode of Chl-*d*

C–H modes of methyl and methylene groups of chlorophylls (and other molecules) are generally found in the 3,000–2,800 cm^{-1} spectral region (Katz et al. 1978; Smith 1999; Socrates 2001). Formyl group C–H stretching is well known to occur at much lower frequencies, however, down to ~2,700 cm^{-1} (Smith 1999; Socrates 2001). For example, Chl-*b* contains a formyl group at the 7^1 position while Chl-*a* contains a methyl group. In IR spectra of Chl-*b*, a band is observed at 2,727 cm^{-1}. No such band is observed in IR spectra of Chl-*a* (Katz et al. 1966, 1978). Accordingly, the 2,727 cm^{-1} band in Chl-*b* FTIR absorbance spectra was assigned to the 7^1 formyl C–H stretching mode.

In our previous work (Sivakumar et al. 2003) ($P740^+$-P740) FTIR DS are presented along with ($P700^+$-P700) FTIR DS, covering the entire 4,000–1,000 cm^{-1} region. Here we are interested in particular in the formyl C–H stretch region (3,000–2,670 cm^{-1}). Figure 2A shows ($P740^+$-P740) FTIR DS in the 3,000–2,670 cm^{-1} region. Figure 2B shows an expanded view of the 2780–2685 cm^{-1} region. The spectra in Fig. 2 are the same as that reported previously (Sivakumar et al. 2003), except here an extended spectral region is shown. The band intensities and noise level in the experiment, as well as the underlying baseline were all considered previously. Several bands are observed in the spectrum in Fig. 2B. In particular negative bands are observed at 2,727 and 2,715 cm^{-1}. No such bands are observed in ($P700^+$-P700) FTIR DS obtained using PS I particles from *S6803* (Sivakumar et al. 2003). This indicates that these bands are likely due to a 3^1 formyl C–H modes of Chl-*d* (Sivakumar et al. 2003). Previously we suggested that the negative band at 2,727 cm^{-1}, could upshift 8 cm^{-1} to 2,735 cm^{-1} upon $P740^+$ formation. However, the 2,727 cm^{-1} band could equally well upshift 26 or 38 cm^{-1} to 2,753 or 2,765 cm^{-1}. The 2,727 cm^{-1} band could also downshift 8, 28 or 38 cm^{-1} to 2,719, 2,699 or 2,689 cm^{-1}, respectively. A second lower intensity negative difference band is observed at 2,715 cm^{-1}. Such a band could suggest the presence of another 3^1 formyl C–H group of Chl-*d*, which is not unreasonable if P740 is dimeric. This 2,715 cm^{-1} band could upshift to 2,719, 2,735 or 2,753 cm^{-1}. It could also downshift to 2,699 or 2,689 cm^{-1}.

There is no experimental data available to indicate how formyl C–H modes of chlorophylls should shift (up or

Fig. 2 ($P740^+$-P740) FTIR DS in the (**A**) 3,000–2,680 cm^{-1} region. (**B**) An expanded view of (A), in the 2,780–2,685 cm^{-1} region. Spectral resolution is 4 cm^{-1}. The spectra shown are the same as that presented previously (Sivakumar et al. 2003), except the wavelength scale has been expanded. All experimental conditions can be found in Sivakumar et al. (2003)

down), and by how much, upon cation formation (FTIR spectroelectrochemistry experiments in the 2,700–3,000 cm^{-1} region are very difficult because of strong solvent absorption). However quantum chemical vibrational frequency calculations for neutral, cation and anion states of chlorophylls can easily be undertaken. In this manuscript we describe the use of such calculations to predict how 3^1 formyl C–H modes of Chl-*d* shift upon radical formation. These predictions can then be used to identify which of the myriad of possible band-shifts in ($P740^+$-P740) FTIR DS (see above) are appropriate.

Figure 1 shows the Chl-*d* model used in our studies, where the phytyl chain has been replaced by a methyl group after the 17^3 ester oxygen. This model is identical to the model molecule studied by Chen et al. (2004). Chl-*d* contains a formyl group rather than a vinyl group at the 3 position, and it is the vibrational properties of this formyl group that distinguish it from Chl-*a*. We have calculated the vibrational frequencies and intensities of all of the normal modes of the model molecule shown in Fig. 1. From these data “stick” spectra are constructed and then convolved with a Gaussian function of 4 cm^{-1} bandwidth to produce more realistic looking IR spectra (Bandaranayake et al. 2006b; Wang et al. 2007), which we will call absorption spectra. Figure 3A shows calculated IR absorbance spectra for Chl-*d*, Chl-d^+ and Chl-d^- in the 3,250–2,820 cm^{-1} region (the spectra are presented at a density of one data point per cm^{-1}). The “cation minus neutral” IR difference spectrum is also shown. No scale factor has been applied to the calculated frequencies. In the C–H region, at this level of calculation [B3LYP 6–31G(d)], a scale factor of 0.962 has been used by others (Chen et al. 2004; Foresman and Frisch 1996). We chose not to scale the frequencies because it is primarily radical induced frequency differences that we are interested in, and these

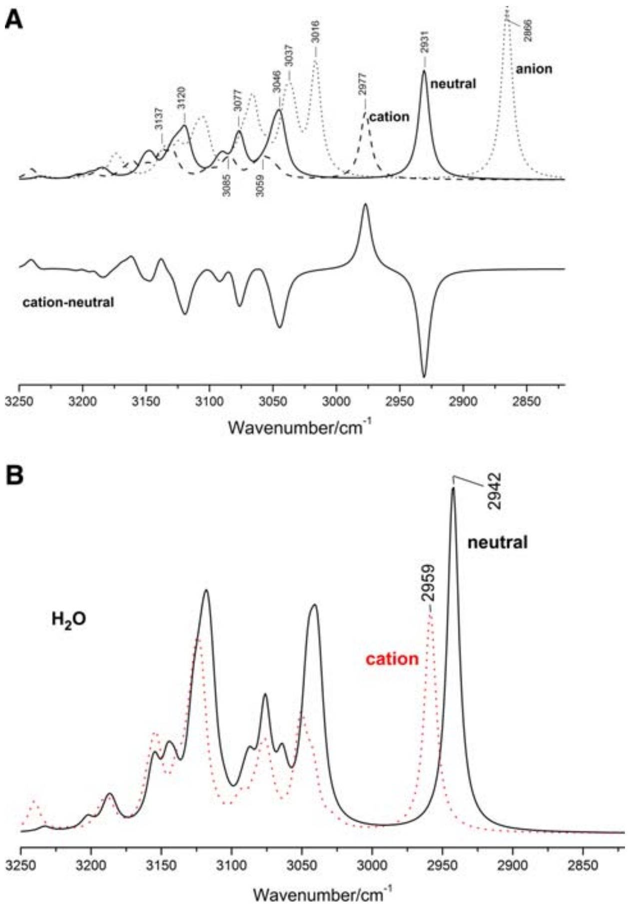

Fig. 3 (**A**) Calculated IR absorption spectra for Chl-*d* (solid line), Chl-d^+ (dashed line) and Chl-d^- (dotted line) in the gas phase. The “cation minus neutral” IR difference spectrum is also shown. (**B**) Calculated IR absorption spectra for Chl-*d* (solid line) and Chl-d^+ (cation—dotted line) in H_2O

differences are accurately calculated without scaling, probably because the same errors are present in both the neutral and radical calculations, and upon subtraction these errors approximately cancel.

The most prominent band in the calculated IR absorbance spectrum of Chl-*d* in Fig. 3A is at 2,931 cm^{-1} and is due to stretching of the C–H group associated with the 3^1 formyl group (Table 1). The hypothesis is that the 2,931 cm^{-1} band in Fig. 3A corresponds to the negative 2,727 cm^{-1} band in Fig. 2B. This would then indicate that the calculated frequencies for the 3^1 formyl C–H modes of Chl-*d* should be scaled by 0.93 (2,727/2,931). A frequency of 2,931 cm^{-1} corresponds to 2,820 cm^{-1} after a scale factor of 0.962 has been applied. In previous work using the same functional and basis set, this mode was calculated to be at 2,814 cm^{-1} after scaling by 0.962 (Chen et al. 2004). The origin of the discrepancy is unclear. It is not clear if Chen et al. (2004) did their calculations at 298 K or 77K. However, we have also undertaken the same calculation at 77 K and find that the 3^1 formyl C–H stretching still occurs at 2,931 cm^{-1} (before scaling). We therefore have no explanation as to why Chen et al. (2004) obtain different calculated results from us. Most likely the Chl-*d* model molecule studied by Chen et al. (2004) is different from ours in some undocumented way. Also, the model for BChl-*a* presented by Chen et al. (2004) is not in fact BChl-*a*. In the supplementary materials section we detail further a comparison of our Raman spectra calculations with that of Chen et al. (2004) and include further details of our calculations at 77 K.

The 2,931 cm^{-1} band in Fig. 3A upshifts 46 cm^{-1} (43 cm^{-1} if a scale factor of 0.93 is used) upon cation formation and decreases in intensity by 39% (Table 1). The calculations also show that the 2,931 cm^{-1} band downshifts 65 cm^{-1} upon anion formation and increases in intensity by 59% (Table 1). Thus for the 3^1 formyl C–H mode of Chl-*d*, the calculations predict the trend of decreasing frequency and increasing intensity as one goes from the cation to neutral to anion state. A similar trend was found for the calculated frequency and intensity of the 13^1 keto C=O group of a Chl-*a* model studied previously, and this is known to accurately reflect experiment (O'Malley 2000; Wang et al. 2007). Since density functional theory based calculations accurately predict the behavior of the 13^1 keto C=O of neutral and radical forms of a Chl-*a* model it is likely that these calculations will also accurately predict the vibrational properties of the 3^1 formyl group of Chl-*d*.

The calculations outlined above were for Chl-*d* in the gas phase. We have also calculated the vibrational properties of Chl-*d* in various solvents, using the integral equation formalism (IEF) of the polarizable continuum model (Cances et al. 1997, 1999; Mennucci and Tomasi 1997; Tomasi et al. 1999, 2002, 2005), as implemented within Gaussian 03. The results of these calculations are summarized in Table 1. Figure 3B also shows calculated spectra for Chl-*d* and Chl-d$^+$ in water.

The 3^1 formyl C–H mode of Chl-*d* in the gas phase upshifts 46 cm^{-1} upon cation formation, and decreases in intensity by 39%. The cation induced frequency upshift of this mode decreases as the dielectric constant of the solvent increases. For example, in CCl_4 the upshift is 35 cm^{-1} while in water the upshift is 17 cm^{-1} (Table 1). In the interior of proteins, such as the environment around the pigments of P740, the dielectric constant is likely to be in the 2–8 range (Dashdorj et al. 2004; Krishtalik 1999). Based on this range, our calculations indicate that the 3^1 formyl C–H mode of Chl-*d* will upshift ~35–23 cm^{-1} upon cation formation (Table 1).

With the calculated results in Table 1 the putative 3^1 formyl C–H bands observed near 2,727 and 2,715 cm^{-1} in

Table 1 Calculated frequencies and intensities (in parenthesis [in km/mole]) for two modes of the 3^1 formyl group of Chl-*d* and Chl-*d*$^+$, obtained using the optimized model molecule shown in Fig. 1

Mode		Neutral ν(I)	Cation ν(I)	Shift (ΔI)	Anion ν(I)	Shift (ΔI)
ν(3^1 C–H)	6-31G(d) Gas	2931(245)	2977(150)	46(−39%)	2866(390)	−65(+59%)
	6-31G(d) H_2O (ε = 78.39)	2942(243)	2959(154)	17(−37%)		
	6-31G(d) THF (ε = 7.58)	2946(269)	2969(164)	23(−39%)		
	6-31G(d) CCl_4 (ε = 2.23)	2939(269)	2974(160)	35(−41%)		
ν(3^1 C=O)	6-31G(d) Gas	1763(369)	1777(232)	14(−37%)	1720(1090)	−43(+195%)
	6-31G(d) H_2O	1725(1018)	1739(736)	14(−28%)		
	6-31G(d) THF	1735(816)	1750(565)	15(−31%)		
	6-31G(d) CCl_4	1750(565)	1764(368)	14(−35%)		

Calculations were undertaken in the gas phase and in three different solvents (using the polarizable continuum model as implemented in Gaussian 03). The dielectric constants for the solvents are 78.39, 7.58 and 2.23 for H_2O, THF and CCl_4, respectively. The cation induced frequency shift of the modes for each calculation is shown along with the mode intensity change [in parenthesis (in %)]. Calculated frequencies and intensities for the two modes of Chl-*d*$^-$ (in the gas phase) are also shown along with the anion induced frequency shift and mode intensity change the (P740$^+$-P740) FTIR DS in Fig. 2B can be reassessed. For example, one concrete calculated result is that the 3^1 formyl C–H modes upshift upon cation formation. Therefore, the band at 2,727 cm^{-1}does not downshift to 2,719, 2,699 or 2,689 cm^{-1}, and the band at 2,715 cm^{-1} does not downshift to 2,699 or 2,689 cm^{-1}.

The calculated IR spectra in Fig. 3A show that there is a correlation between the charge on the Chl-*d* pigment and the frequency of the formyl C–H mode. The more positive the charge on the pigment, the higher the frequency of the 3^1 formyl C–H mode. Assuming an effective dielectric constant of about 2.23 near the pigments of P740, if one unit of positive charge on Chl-*d* causes a 35 cm^{-1} increase in frequency of the 3^1 formyl C–H mode then one half unit of charge on Chl-*d* will very roughly cause a 17.5 cm^{-1} increase in frequency. That is, if P740 consists of two Chl-*d* molecules in an environment of low effective dielectric constant, and in the P740$^+$ state the charge is distributed evenly between the pigments, then we may expect a cation induced upshift of two 3^1 formyl C–H modes by ~17.5 cm^{-1}. Previously we hypothesized that the 2,727 cm^{-1} band could upshift 8 cm^{-1} to 2,735 cm^{-1} upon cation formation. An 8 cm^{-1} cation induced increase in frequency of the 3^1 formyl C–H mode would then indicate ~23% of the charge resides on one of the pigments of P740. However, the 2,727 cm^{-1} band is more intense than the other bands in this spectral region, indicating that it is likely associated with the pigment of P740 that carries more of the charge. The intensity of the 2,727 cm^{-1} band, along with the calculations summarized in Table 1, indicate that the 2,727 cm^{-1} band cannot upshift only 8 cm^{-1} upon cation formation (the same kind of conclusions are still valid, even for a dielectric constant of 78 [water]). Therefore, from the (P740$^+$-P740) FTIR DS in Fig. 2B, the 2,727 cm^{-1} band must upshift 26 or 38 cm^{-1} to 2,753 or 2,765 cm^{-1}, respectively. An upshift of 38 cm^{-1} would indicate that all of the charge is on a single Chl-*d* pigment, and that the dielectric environment around this pigment is below ~2. This is unlikely given the presence of the 2,715 cm^{-1} band in the (P740$^+$-P740) FTIR DS. Therefore, the calculations predict that the 2,727 cm^{-1} band upshifts ~26 cm^{-1} to 2,753 cm^{-1} upon cation formation. Similarly the calculations predict that the 2,715 cm^{-1} band upshifts ~20 cm^{-1} to 2,735 cm^{-1} (and not 38 cm^{-1}–2753 cm^{-1}). Based on the experimental data in Fig. 2B, the calculations predict that (1) P740 consists of two Chl-*d* molecules, (2) the effective dielectric environment around the two Chl-*d* pigments of P740 is very low and (3) in the P740$^+$ state, charge is asymmetrically distributed over the two Chl-*d* pigments (to a very rough approximation, ~60/40%). Mino et al. (2005) suggest that the spin density distribution over the Chl-*d* pigments in the P740$^+$ state is quite asymmetric, as is also found to be the case for the spin density distribution over the Chl-*a* pigments in the P700$^+$ state (Webber and Lubitz 2001). The relationship between intermolecular spin and charge distributions is not precise, and it has been suggested that a largely symmetric charge distribution over the pigments in the P700$^+$ state (Breton et al. 1999) is not necessarily incompatible with the highly asymmetric spin distribution estimates derived from ENDOR spectroscopy of P700$^+$ (Lubitz 2006; Plato et al. 2003). Therefore, the suggested asymmetric spin density distribution over the Chl-*d* pigments in the P740$^+$ state (Mino et al. 2005) may not be incompatible with our quite symmetric estimation of the charge density distribution over the pigments in the P740$^+$ state.

A rather symmetric charge distribution over the pigments in the P740$^+$ state is compatible with other aspects of the (P740$^+$-P740) FTIR DS. For instance the (P740$^+$-P740) FTIR DS display a broad, structured, positive, IR band in the 2,000–3,500 cm^{-1} region that indicates that the P740$^+$ state is delocalized over at least two pigments (Sivakumar et al. 2003). This broad band displays a shoulder near 2,250 cm^{-1}, and is overall very similar to the corresponding band found in ($P^+Q_A^-PQ_A$) FTIR DS obtained using purple bacterial reaction centers from *R. sphaeroides* (Breton et al. 1992; Johnson et al. 2002). The presence of the shoulder near 2,250 cm^{-1} is suggestive that the charge is delocalized over the Chl-*d* pigments in a manner similar to that in *R. sphaeroides* RCs, which is roughly 2:1 favoring the L branch (Johnson et al. 2002).

Chlorophyll methyl and methylene C–H stretching vibrations

In Fig. 3A, for the neutral state of Chl-*d*, the band peaking at 3,046 cm^{-1} is due to the overlap of nine bands that are due to C–H stretching of methyl and methylene groups of Chl-*d*. Some of the modes that contribute to the 3,046 cm^{-1} neutral state band also contribute to the 3,059 cm^{-1} band of the cation state. We therefore conclude that the 3,046 cm^{-1} band is due to C–H modes of methyl and methylene groups of Chl-*d*, and that it upshifts ~13 cm^{-1} to 3,059 cm^{-1} upon cation formation. Similarly, the 3,077 and 3,120 cm^{-1} bands upshift 13 and 17 cm^{-1} upon cation formation, respectively. Notice that these C–H modes also decrease in intensity by more than a factor of two upon cation formation. These calculated results agree well with experimental trends found in both (P700$^+$-P700) (Sivakumar et al. 2003) and (P740$^+$-P740) FTIR DS (Fig. 2A). For example, we can unambiguously conclude that the 2,957 cm^{-1} band upshifts 15 cm^{-1} to 2972 cm^{-1} upon cation formation. Similarly, the calculations indicate that the bands at 2,929, 2,917 and 2,828 cm^{-1} can be interpreted in terms of upshifting 14, 20 and 16 cm^{-1} to 2,943, 2,937 and 2,844 cm^{-1} upon P740$^+$

formation. In addition, these bands clearly decrease in intensity upon cation formation, as predicted.

In Fig. 3A it is also apparent that that the band associated with the 3^1 formyl C–H stretch is considerably more intense than the higher frequency bands associated with methyl and methylene C–H modes. This is not in line with the experimental data in Fig. 2A, which show the methyl and methylene bands are more intense than the bands associated with the C–H mode of the 3^1 formyl group of Chl-*d* (compare the cation—neutral spectrum in Fig. 3A with the corresponding spectrum in Fig. 2A). At present, it is not entirely clear how to rationalize this difference between experiment and calculation.

The 3^1 formyl C=O mode of Chl-*d*

Table 1 shows that the 3^1 formyl C=O mode of Chl-*d* in the gas phase is calculated to occur at 1,763 cm^{-1}. No scale factor has been applied to this calculated frequency. At this level of calculation [B3LYP 6–31G(d)], a scale factor of 0.94 has been used by others (Chen et al. 2004; Foresman and Frisch 1996). Applying such a scale factor, we would predict the 3^1 formyl C=O mode of Chl-*d* in the gas phase at 1,657 cm^{-1}. Raman spectra of Chl-*d* in acetonitrile at 77 K have suggested that a band at 1,659 cm^{-1} is due to the 3^1 formyl C=O mode of Chl-*d*.

Using the integral equation formalism of the polarizable continuum model within Gaussian 03, we see that the calculated frequency of the 3^1 formyl C=O mode of Chl-*d* is strongly dependant on the solvent dielectric constant, ranging from 1,750 cm^{-1} (1,645 cm^{-1} after scaling) in CCl_4 to 1,725 cm^{-1} (1,622 cm^{-1} after scaling) in water. The 3^1 formyl C=O mode intensity also increases considerably as the solvent dielectric constant increases (Table 1). Upon cation formation the 3^1 formyl C=O mode of Chl-*d* upshift 14–15 cm^{-1}, independent of the dielectric constant. These predicted result concerning cation induced frequency and intensity changes for the 3^1 formyl C=O mode of Chl-*d* cannot easily be compared to bands in the (P740$^+$-P740) FTIR DS, simply because no bands in the experimental spectrum have been unambiguously associated with the 3^1 formyl C=O mode of Chl-*d* molecules (Sivakumar et al. 2003). However, we expect that these calculated predictions for the 3^1 formyl C=O mode of Chl-*d* will be useful in future FTIR studies of isotope labeled PS I from *A. marina*.

The primary donor in *A. marina* PS II Particles

Very recently, a FTIR DS associated with the putative primary electron donor in PS II particles from *A. marina* has been reported (Tomo et al. 2007). This donor, called P713, was suggested to consist of two Chl-*d* molecules. This hypothesis was based on the observation of two negative bands at 2,723 and 2,696 cm^{-1} in the (P713$^+$-P713) FTIR DS. Notably, however, no corresponding positive bands were observed in the (P713$^+$-P713) FTIR DS. This may be an indication that the bands at 2,723 and 2,696 cm^{-1} are not associated with pigments of the primary donor. Rather the two bands may be due to an electrochromic effect on the 3^1 formyl C–H group of Chl-*d* pigments that are near the oxidized donor. If this is the case, P713 need not be interpreted as a dimer of Chl-*d* pigments. Intriguingly, recent visible absorption difference spectroscopy measurements on *A. marina* PS II particles suggest that the positive charge may be localized on a single Chl-*a* molecule (Schlodder et al. 2007). In any case, more detailed (P713$^+$-P713) FTIR DS covering the whole of the 4,000–2,000 cm^{-1} region will be required before more concrete conclusions can be drawn.

Conclusions

DFT based vibrational mode frequency calculations for Chl-*d* show that the 3^1 formyl C–H mode upshifts upon cation formation. This prediction alone limits the number of possible interpretations on bands in (P740$^+$-P740) FTIR DS. It is found that the 3^1 formyl C–H mode of Chl-*d* upshifts up to 46 cm^{-1} upon cation formation, depending on the dielectric constant of the solvent used in the calculation. This calculated result further limits the number of possible interpretations on bands in (P740$^+$-P740) FTIR DS. Considering the calculated spectra, only a single self consistent interpretation of how bands associated with 3^1 formyl C–H modes of Chl-*d* shift in (P740$^+$-P740) FTIR DS can be drawn. The calculations are therefore shown to be of great value for interpretation of how bands shift in FTIR DS upon radical formation. Specifically, our calculations in combination with (P740$^+$-P740) FTIR DS indicate that P740 is a dimeric Chl-*d* species, in an environment of low effective dielectric constant (~2–8). In the P740$^+$ state, charge is asymmetrically distributed over the two Chl-*d* pigments (~60/40).

Acknowledgments This work was supported by the National Research Initiative of the USDA Cooperative State Research Education and Extension Service grant number 2004-35318-14889, and NSF grant number DBI: 0352324 to GH. RW was supported by a fellowship from the Molecular Basis of Disease Program at Georgia State University.

References

Akiyama M et al (2001) Detection of chlorophyll *d*’ and pheophytin a in a chlorophyll *d*-dominating oxygenic photosynthetic prokaryote *Acaryochloris marina*. Anal Sci 17(1):205–208

Akiyama M et al (2002a) Detection of chlorophyll d' and pheophytin a in a chlorophyll *d*-dominating oxygenic photosynthetic prokaryote *Acaryochloris marina*. Plant Cell Physiol 43:S170

Akiyama M et al (2002b) Quest for minor but key chlorophyll molecules in photosynthetic reaction centres—unusual pigment composition in the reaction centers of the chlorophyll *d*-dominated cyanobacterium *Acaryochloris marina*. Photosynth Res 74(2):97–107

Bandaranayake K et al (2006a) Modeling the A_1 binding site in photosystem I. Density functional theory for the calculation of "anion—neutral" FTIR difference spectra of phylloquinone. Vib Spectrosc 42(1):78–87

Bandaranayake KMP et al (2006b) Modification of the phylloquinone in the A_1 binding site in photosystem I studied using Time-Resolved FTIR difference spectroscopy and density functional theory. Biochemistry 45(16):4121–4127

Breton J et al (1992) A new infrared electronic-transition of the oxidized primary electron-donor in bacterial reaction centres—a way to assess resonance interactions between the bacteriochlorophylls. Biochem 31(33):7503–7510

Breton J et al (1999) FTIR study of the primary electron donor of photosystem I (P700) revealing delocalization of the charge in P700(+) and localization of the triplet character in (3)P700. Biochem 38(36):11585–11592

Cances E et al (1997) A new integral equation formalism for the polarizable continuum model: theoretical background and applications to isotropic and anisotropic dielectrics. J Chem Phys 107(8):3032–3041

Cances E et al (1999) Integral equation methods for molecular scale calculations in the liquid phase. Math Models Methods Appl Sci 9(1):35–44

Chen M et al (2004) Raman properties of chlorophyll *d*, the major pigment of *Acaryochloris marina*: studies using both Raman spectroscopy and density functional theory. Spectrochim Acta A Mol Biomol Spectrosc 60(3):527–534

Dashdorj N et al (2004) Electrochromic shift of chlorophyll absorption in photosystem I from *Synechocystis* sp. PCC 6803: a probe of optical and dielectric properties around the secondary electron acceptor. Biophys J 86(5):3121–3130

Foresman J, Frisch A (1996) Exploring chemistry with electronic structure methods, 2nd edn. Gaussian Inc., Pittsburg, PA

Frisch MJ et al (2004) Gaussian 03, Revision C.02

Hastings G (2001) Time-resolved step-scan Fourier transform infrared and visible absorption difference spectroscopy for the study of photosystem I. Appl Spectrosc 55(7):894–900

Heald RL et al (1988) Resonance Raman spectra of electrochemically generated chlorophyll a cation radical. J Phys Chem 92(17):4820–4824

Hu Q et al (1998) A photosystem I reaction center driven by chlorophyll *d* in oxygenic photosynthesis. Proc Natl Acad Sci USA 95(22):13319–13323

Johnson ET et al (2002) Electronic and vibronic coupling of the special pair of bacteriochlorophylls in photosynthetic reaction centers from wild-type and mutant strains of *Rhodobacter sphaeroides*. J Phys Chem B 106(45):11859–11869

Katz JJ et al (1966) Infrared and nuclear magnetic resonance spectroscopy of chlorophyll. In: Vernon LP, Seely GR (eds) The chlorophylls. Academic Press, New York

Katz JJ et al (1978) Chlorophyll agregation: coordination interactions in chlorophyll monomers, dimers and oligomers. In: Dolphin D (ed) The porphyrins. Physical Chemistry, Part C, Academic Press

Krishtalik LI (1999) Role of the protein's low dielectric constant in the functioning of the photosynthetic reaction center. Photosyn Res 60(2–3):241–246

Lubitz W (2006) EPR studies of the primary electron donor P700 in photosystem I. In: Golbeck J (ed) Photosystem I: the light driven plastocyanin: Ferredoxin oxidoreductase. Springer

Mennucci B, Tomasi J (1997) Continuum solvation models: a new approach to the problem of solute's charge distribution and cavity boundaries. J Chem Phys 106(12):5151–5158

Mino H et al (2005) Proton ENDOR study of the primary donor P740(+), a special pair of chlorophyll *d* in photosystem I reaction center of *Acaryochloris marina*. Chem Phys Lett 411(1–3):262–266

Miyashita H et al (1996) Chlorophyll *d* as a major pigment. Nature 383(6599):402–402

Miyashita H et al (1997) Pigment composition of a novel oxygenic photosynthetic prokaryote containing chlorophyll *d* as the major chlorophyll. Plant Cell Physiol 38(3):274–281

Nabedryk E et al (1990) Fourier transform infrared difference spectroscopy shows no evidence for an enolization of chlorophyll *a* upon cation formation either in vitro or during P700 photooxidation. Biochem 29(13):3242–3247

O'Malley P (2000) The effect of oxidation and reduction of chlorophyll *a* on its geometry, vibrational and spin density properties as revealed by hybrid density functional methods. J Am Chem Soc 122(32):7798–7801

Plato M et al (2003) Molecular orbital study of the primary electron donor P700 of photosystem I based on a recent X-ray single crystal structure analysis. Chem Phys 294(3):483–499

Schlodder E et al (2007) Both chlorophylls *a* and *d* are essential for the photochemistry in photosystem II of the cyanobacteria, *Acaryochloris marina*. Biochim Biophys Acta 1767(6):589–595

Sivakumar V et al (2003) Photo-oxidation of P740, the primary electron donor in photosystem I from *Acaryochloris marina*. Biophys J 85(5):3162–3172

Smith BC (1999) Infrared spectral interpretation: a systematic approach. CRC Press, Boca Raton

Socrates G (2001) Infrared and Raman characteristic group frequencies. Tables and Charts. Wiley. Chichester, New York

Tomasi J et al (1999) The IEF version of the PCM solvation method: an overview of a new method addressed to study molecular solutes at the QM ab initio level. J Mol Struct Theochem 464(1–3):211–226

Tomasi J et al (2002) Molecular properties in solution described with a continuum solvation model. Phys Chem Chem Phys 4(23):5697–5712

Tomasi J et al (2005) Quantum mechanical continuum solvation models. Chem Rev 105(8):2999–3093

Tomo T et al (2007) Identification of the special pair of photosystem II in a chlorophyll *d*-dominated cyanobacterium. Proc Natl Acad Sci USA 104(17):7283–7288

Wang R et al (2007) Density functional theory based calculations of the vibrational properties of chlorophyll-*a*. Vib Spectrosc 44:357–368

Webber AN, Lubitz W (2001) P700: the primary electron donor of photosystem I. Biochim Biophys Acta 1507(1–3):61–79

Wheeler RA (2001) Quinones and quinoidal radicals in photosynthesis. In: Eriksson LA (ed) Theoretical Biochemistry-processes and properties of biological systems. Elsevier